Available online at www.synsint.com

Synthesis and Sintering

ISSN 2564-0186 (Print), **ISSN** 2564-0194 (Online)

Research article

Effect of ZnO particle size on the sintering behavior, phase evolution, and optical properties of transparent borosilicate glazes

Raziye Salami, Aida Faeghinia *, Zahra Khakpour, Mohammad Zakeri

Ceramics Department, Materials and Energy Research Center (MERC), Karaj, Iran

ABSTRACT

This study investigates the influence of zinc oxide (ZnO) particle size on the properties of SiO_2–Al_2O_3–B_2O_3–ZnO–CaO–K_2O transparent glass–ceramic glazes. Two ZnO sources were employed, including synthesized nano-sized ZnO (~500 nm) and commercial micro-sized ZnO (>1 μm). The results indicate that nano-sized ZnO enhances melting reactivity and modifies the crystallization behavior of the glaze systems compared with micro-sized ZnO. X-ray diffraction (XRD) and scanning electron microscopy (SEM) analyses revealed differences in phase evolution and crystal morphology depending on ZnO particle size. Nano-sized ZnO promoted finer and more homogeneous crystalline distributions, while micro-sized ZnO resulted in coarser crystalline structures. Furthermore, the optical and surface properties of the glazes were strongly influenced by the balance between densification and crystallization during firing. The results demonstrate that ZnO particle size plays a significant role in controlling the thermal behavior, phase evolution, microstructure, and surface quality of transparent borosilicate glazes.

KEYWORDS

Zinc oxide
Glass-ceramic glazes
Crystallization behavior
Microstructure evolution
Borosilicate glass system
Transparent ceramics

OPEN ACCESS

1. Introduction

Transparent borosilicate glazes are widely used in ceramic tile applications because of their favorable combination of chemical durability, thermal stability, surface gloss, and optical transparency. The performance of these glaze systems is strongly dependent on the relationship between glass composition, crystallization tendency, sintering behavior, and microstructural development during firing. In transparent glaze systems, the control of crystallization and residual porosity is particularly important because even limited phase separation, devitrification, or trapped porosity can significantly reduce transparency and surface quality [1, 2].

Among the different oxides used in glaze technology, ZnO plays a critical role in controlling both the thermal and structural behavior of silicate-based glass systems. ZnO acts as an intermediate oxide and, depending on concentration and glass composition, may behave either as a network modifier or as a partial network former [3, 4]. In ceramic glazes, ZnO is known to reduce melt viscosity, improve surface gloss, enhance chemical durability, and influence crystallization behavior. In ZnO-containing glass–ceramic glaze systems, crystalline phases such as willemite (Zn_2SiO_4) and gahnite ($ZnAl_2O_4$) may form during thermal treatment, leading to substantial changes in mechanical and optical properties [5, 6].

The crystallization behavior of ZnO-containing glazes is closely associated with the kinetics of nucleation and crystal growth during firing. Previous studies have shown that the morphology and distribution of Zn-containing crystalline phases strongly depend on the viscosity of the residual glass phase, thermal history, and chemical composition of the glaze system. Furthermore, the formation of

* Corresponding author. *E-mail address:* a.faeghinia@merc.ac.ir (A. Faeghinia)
Received 22 July 2025; Received in revised form 18 March 2026; Accepted 18 March 2026.

https://doi.org/10.53063/synsint.2026.61300

crystalline phases during firing can either improve or deteriorate glaze performance depending on the extent of crystallization and the resulting microstructure. Excessive crystallization or heterogeneous crystal growth may increase light scattering and reduce transparency, whereas controlled crystallization can improve hardness and surface stability [7–9].

In recent years, increasing attention has been directed toward the use of nano-sized particles in ceramic and glass–ceramic systems. Nanometric powders possess significantly larger specific surface area and higher surface energy compared with conventional micro-sized powders. As a result, particle size can substantially influence melting kinetics, diffusion behavior, viscous flow sintering, and crystallization mechanisms during thermal processing. In glaze systems, finer particles may accelerate densification and modify nucleation behavior because of increased contact area between particles and enhanced reactivity [10–13]. The influence of particle size on sintering and crystallization is particularly important in transparent glaze systems. Faster densification can reduce residual porosity and improve optical transmission; however, excessive surface crystallization may inhibit viscous flow and lead to incomplete sintering or increased opacity. Therefore, optimization of particle size is essential to balance densification, phase evolution, and optical performance [14–16].

ZnO particle size is also associated with changes in the thermal stability of glass systems. Variations in glass transition temperature, crystallization temperature, and glass-forming ability may occur because of differences in dissolution kinetics and structural interactions between ZnO and the silicate network. These structural modifications can subsequently influence the formation of wollastonite, willemite, calcium aluminosilicate, and other crystalline phases during firing [17–19].

Although the role of ZnO in glaze chemistry has been extensively discussed, the specific effect of ZnO particle size on the thermal behavior, crystallization tendency, microstructural development, and optical properties of transparent borosilicate glazes remains insufficiently understood. In particular, comparative investigations between nano-sized and micro-sized ZnO sources in transparent glaze systems remain limited [20–22].

The present study investigates the influence of ZnO particle size on the sintering behavior, phase evolution, and optical properties of transparent borosilicate glazes prepared in the SiO_2–Al_2O_3–B_2O_3–ZnO–K_2O–CaO system. Two ZnO powders with different particle sizes, including nano-sized ZnO (~500 nm) and micro-sized commercial ZnO (>1 μm), were employed as raw materials. The effects of particle size on thermal behavior, glass stability, crystallization, microstructure, hardness, and optical characteristics were systematically evaluated using DTA, FTIR, XRD, SEM, and colorimetric analyses.

2. Experimental procedure

2.1. Synthesis of nano-sized ZnO powder

The nano-sized zinc oxide (ZnO) used in this study was synthesized through a recovery process from industrial waste, specifically zinc smelting filter cake. The synthesis procedure involved the following steps: (i) Leaching and purification: The initial precursor (zinc filter cake) underwent a hydrometallurgical treatment. It was subjected to acidic leaching using sulfuric acid to dissolve zinc ions, followed by a multi-stage purification process to eliminate metallic impurities such as iron (Fe) and cadmium (Cd). (ii) Precipitation: To obtain the zinc precursor, sodium carbonate was added to the purified zinc sulfate solution under controlled pH conditions. This resulted in the precipitation of zinc carbonate ($ZnCO_3$) or basic zinc carbonate. (iii) Calcination: The obtained precipitate was filtered, washed repeatedly with deionized water to remove residual salts, and then dried. The final conversion to nano-sized ZnO was achieved through a controlled calcination process at 600 °C for 2 h in a muffle furnace.

2.2. Frit preparation and glaze formulation

The transparent glass-ceramic glazes were investigated within the SiO_2–Al_2O_3–B_2O_3–ZnO–K_2O–CaO borosilicate chemical system. The raw materials, including high-purity quartz, kaolin, boric acid, calcium carbonate, and potassium carbonate, were precisely weighed according to the predetermined formulations (Table 1). Hereafter, the ratio K_2O/(CaO + ZnO) is referred to as the S ratio. To evaluate the impact of zinc oxide particle size, two comparative experimental series were designed: the F-series (utilizing commercial micro-sized ZnO) and the N-series (utilizing synthesized nano-sized ZnO).

The starting batches were thoroughly homogenized via a dry ball milling process using alumina media to ensure a uniform distribution of the precursors. The mixtures were then transferred into high-purity alumina crucibles and melted in an electric furnace at temperatures ranging from 1450 °C to 1550 °C. To obtain the frit, the refined molten glass was rapidly quenched in distilled water, followed by drying and subsequent pulverization.

2.3. Slip preparation

To prepare a stable glazing slip, the obtained frits were wet-milled with 0.5 wt% kaolin as a suspending agent and 0.1 wt% carboxymethyl cellulose (CMC) as a temporary binder. The density of the slurry was precisely adjusted and maintained at 1.75 g/cm^3 to optimize the rheological properties for coating. The formulated slips were uniformly applied onto standard porcelain substrates using the industrial bell-coating technique. To study the sintering behavior and phase evolution under realistic industrial conditions, the green-coated samples were

Table 1. Weight percentages of oxides used in the samples.

Sample	K_2O	SiO_2	Al_2O_3	B_2O_3	CaO	ZnO	K_2O/(CaO + ZnO)
F1, N1	7.5	60.1	8.2	4.2	12.7	7.1	0.37
F2, N2	6.5	60.1	8.2	4.2	15.2	5.8	0.31
F3, N3	3.5	61.67	8.2	4.2	17.7	4.3	0.27

fired in an industrial-scale roller kiln at a peak temperature of 1060 °C with a rapid total firing cycle of 45 minutes.

2.4. Characterization

The structural units and chemical bonding configurations within the borosilicate glass network were monitored using Fourier transform infrared spectroscopy (FTIR) (Model: Nexus 670, Thermo Nicolet) in the specific wavenumber range of 400–1400 cm^{-1}. The phase evolution, crystal growth, and identification of the precipitated crystalline phases (such as willemite) were determined via X-ray diffraction (XRD: PHILIPS PW1730). The microstructural morphology, crystal size, and elemental distribution of the fired glaze surfaces were examined using field emission scanning electron microscopy (FE-SEM: MIRA3 TESCAN) coupled with energy dispersive X-ray spectroscopy (EDS).

To quantify the optical properties, the surface gloss was evaluated using a tri-angle gloss meter at a geometry of 60 °, while the chromatic coordinates (L*, a*, b*) were measured using a spectrophotometer according to the CIE Lab system. Finally, the surface mechanical performance was assessed by measuring the microhardness via the Vickers indentation method.

3. Results and discussion

3.1. Thermal behavior and glass stability

The thermal behavior of the prepared borosilicate glass systems was investigated using DTA analysis in order to evaluate the influence of ZnO particle size on glass transition, crystallization tendency, and thermal stability. The DTA curves of all investigated systems are presented in Fig. 1 and reveal distinct differences between glazes prepared using nano-sized ZnO and those prepared using micro-sized commercial ZnO.

The thermal parameters extracted from the DTA curves are summarized in Table 2 and demonstrate that both composition and ZnO particle size strongly affect the thermal response of the glasses.

The results show that decreasing the S ratio resulted in a gradual increase in the glass transition temperature (T_g) and crystallization temperature (T_p), indicating structural modifications within the borosilicate glass network. This behavior indicates progressive modification of the borosilicate network structure and increasing thermal stability against premature crystallization.

In the micro-sized ZnO systems (F-series), the increase in T_p with decreasing S ratio suggests suppression of crystal nucleation during heating. However, the nano-sized ZnO systems exhibited a different tendency, particularly in the N3 composition where the thermal stability parameter decreased relative to the corresponding F3 sample. This result indicates that nano-sized ZnO promotes crystallization kinetics because of its higher surface area and greater reactivity during glass formation.

The enhanced reactivity of nano-sized ZnO likely facilitates the formation of Zn-rich structural domains during melting. These domains can subsequently act as effective nucleation centers during heating, accelerating crystallization processes. The broader crystallization exotherms observed in the nano-sized ZnO systems may indicate overlapping crystallization events and wider distributions of crystal growth behavior. This observation is consistent with the phase evolution and microstructural differences observed in the XRD and SEM analyses. The differences between F-series and N-series samples confirm that ZnO particle size not only affects melting behavior, but fundamentally alters nucleation mechanisms and thermal evolution of the glass network.

3.2. FTIR investigation

Fourier transform infrared spectroscopy (FTIR) was conducted within the specific wavenumber range of 400–1400 cm^{-1} to explore the internal structural modifications and structural groups of the borosilicate glass framework. The results are shown in Fig. 2. The absorption bands observed between 400 and 1200 cm^{-1} correspond primarily to Si–O–Si bending and stretching vibrations together with Zn–O-related structural units. The broad band around 1000–1100 cm^{-1} is associated with asymmetric stretching vibrations of silicate tetrahedra, while the lower-frequency region reflects bending modes and structural rearrangements within the borosilicate network.

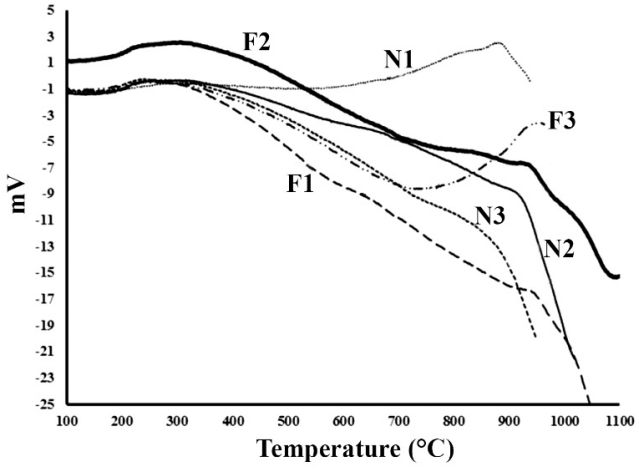

Fig. 1. DTA curves of F1–F3 and N1–N3 glass systems.

Table 2. Glass transition temperature (T_g), crystallization temperature (T_p), and glass stability parameters calculated from DTA curves.

Sample	T_g (°C)	T_p (°C)	T_p - T_g
F1	618	928	310
F2	704	930	226
F3	772	945	173
N1	594	889	295
N2	690	916	226
N3	725	860	135

The results indicate that decreasing the S ratio increases the intensity of bands associated with ZnO_4 structural units. This behavior suggests stronger participation of Zn ions in the glass network. In borosilicate glasses, Zn may act as either a modifier or intermediate oxide depending on local coordination and composition.

The increased intensity of bands associated with Zn-containing structural units suggests stronger interaction between Zn ions and the borosilicate network in the nano-sized ZnO systems. The enhanced dissolution behavior of finer ZnO particles may promote structural depolymerization, which can influence melt viscosity, atomic mobility, and subsequent crystallization behavior during firing. The formation of Zn-containing structural units may also be associated with the crystallization behavior observed during heat treatment. Consequently, the FTIR results provide strong evidence linking ZnO particle size with phase evolution behavior observed in the XRD analyses.

3.3. Sintering and densification behavior

The sintering behavior of the transparent borosilicate glazes prepared with varying particle sizes of zinc oxide (ZnO) was monitored through industrial roller kiln firing profiles. Sintering in glass-ceramic glazes primarily proceeds via viscous flow sintering, where the decrease in viscosity allows surface tension forces to eliminate porosity and maximize densification. Surface defects observed in fired glazes under unsuitable thermal conditions are shown in Fig. 3. The experimental observations indicate that the incorporation of nano-sized ZnO significantly enhances the sintering kinetics compared to the commercial micro-sized ZnO powders (F-series).

The nano-sized ZnO particles possessed a higher specific surface area, which promoted faster diffusion and structural rearrangement within the glaze matrix. As a result, viscous flow densification occurred at a noticeably accelerated rate compared to micro-sized ZnO systems. This enhanced kinetic behavior promoted earlier densification during the initial heating stage, particularly in the nano-ZnO (N-series) samples during firing up to 1060 °C. However, the same high reactivity of nano-ZnO also increased the tendency for crystallization during thermal treatment. In cases where crystallization initiated before complete viscous flow densification, rigid crystalline domains formed within the glaze structure, hindering further densification. This competition between viscous flow and crystallization resulted in residual porosity and surface heterogeneities observed in several samples, highlighting the sensitivity of the system to thermal processing conditions. Therefore, optimization of firing temperature and soaking time was found to be essential in achieving a balance between densification and crystallization. While excessively low temperatures led to incomplete melting and insufficient surface leveling, overly high temperatures promoted uncontrolled crystallization and loss of transparency. In contrast, micro-ZnO (F-series) required higher thermal energy to reach a comparable degree of structural integration, and under rapid industrial firing cycles, occasionally retained minor surface defects due to incomplete healing. Overall, the results demonstrate that particle size plays a critical role in controlling the kinetic competition between viscous flow and crystallization in ZnO-containing glaze systems. The densification behavior of the nano-sized systems demonstrates that particle size affects not only melting kinetics but also the sequence of thermal events occurring during glaze formation.

3.4. Phase evolution and crystallization kinetics

The phase evolution and crystal growth within the fired transparent glazes were evaluated utilizing X-ray diffraction (XRD). The primary objective was to observe the structural transition from a fully amorphous glass matrix to a controlled glass-ceramic structure containing crystalline phases. Fig. 4 shows the formation of an amorphous phase during powder preparation, with no evidence of crystallization.

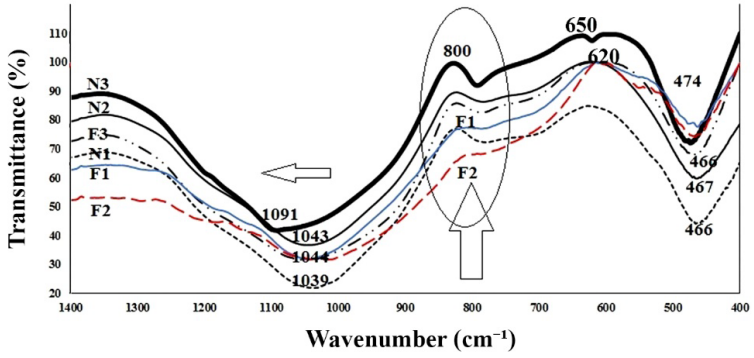

Fig. 2. FTIR spectra of F1–F3 and N1–N3 glass systems.

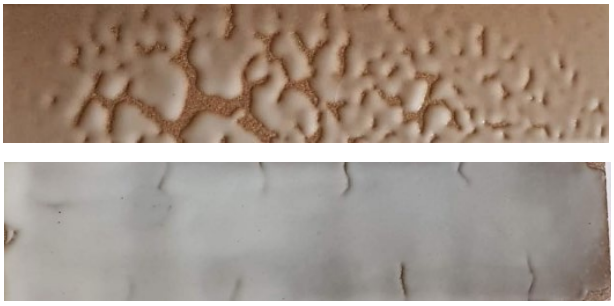

Fig. 3. Surface defects observed in fired glazes under unsuitable thermal conditions, including pore formation and incomplete surface leveling.

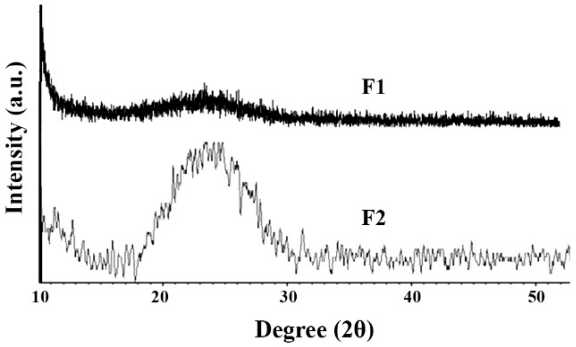

Fig. 4. XRD patterns of frit showing formation of amorphous phase.

The XRD results, shown in Fig. 5, reveal that multiple crystalline phases formed depending on both composition and ZnO particle size. The primary phases identified include wollastonite ($CaSiO_3$), willemite (Zn_2SiO_4), calcium silicate, and calcium aluminosilicate compounds. The micro-sized ZnO systems generally exhibited weaker willemite crystallization compared with the nano-sized systems. This result suggests that nano-sized ZnO facilitates more effective interaction between Zn and silicate structural units during firing. In the N-series samples, willemite crystallization became particularly pronounced. The enhanced formation of willemite can be attributed to improved dissolution and dispersion of ZnO throughout the glass matrix. Nano-sized particles increase contact area and reduce diffusion distances, thereby accelerating Zn–Si interactions during heat treatment. The formation of wollastonite phases was additionally observed in several compositions.

Wollastonite formation is important because acicular wollastonite crystals may significantly influence both hardness and optical properties. Although wollastonite improves mechanical strength, excessive crystal growth can increase light scattering and reduce transparency. The coexistence of wollastonite and willemite indicates simultaneous participation of CaO and ZnO in crystallization reactions. The competition between these crystalline phases depends strongly on local composition and thermal history. The XRD patterns additionally demonstrate that the nano-sized systems exhibit higher overall crystallization intensity. This observation confirms that ZnO particle size acts as a major controlling factor for nucleation kinetics in transparent borosilicate glaze systems.

3.5. Microstructural evaluation

To visually correlate the sintering and crystallization kinetics with spatial morphology, FE-SEM coupled with EDS analysis was conducted on the cross-sections and surface configurations of the fired glazes. As shown in Fig. 6, the microstructural micrographs revealed a profound contrast in crystal size and spatial distribution between the F-series and N-series samples.

Needle-like willemite crystals can also be observed in the F2 and N2 samples. The spherical morphologies observed in the F3 and N3 samples may be associated with the formation of anorthite and parawollastonite-related phases, respectively. These differences may additionally be influenced by compositional variations associated with lower K_2O contents and local structural changes during firing.

FE-SEM images of the microstructure of samples in higher magnification are displayed in Fig. 7. The N-series samples demonstrated a comparatively more homogeneous microstructure characterized by finer crystalline features distributed within the residual glass matrix. The reduced crystal size and more uniform distribution may contribute to lower optical scattering compared with the coarse crystalline aggregates observed in the F-series samples.

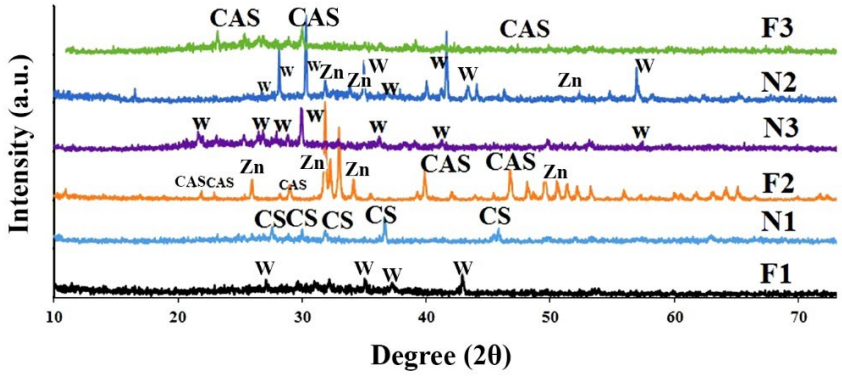

Fig. 5. XRD patterns of glazes fired at 1060 °C showing crystallization evolution after glaze firing.

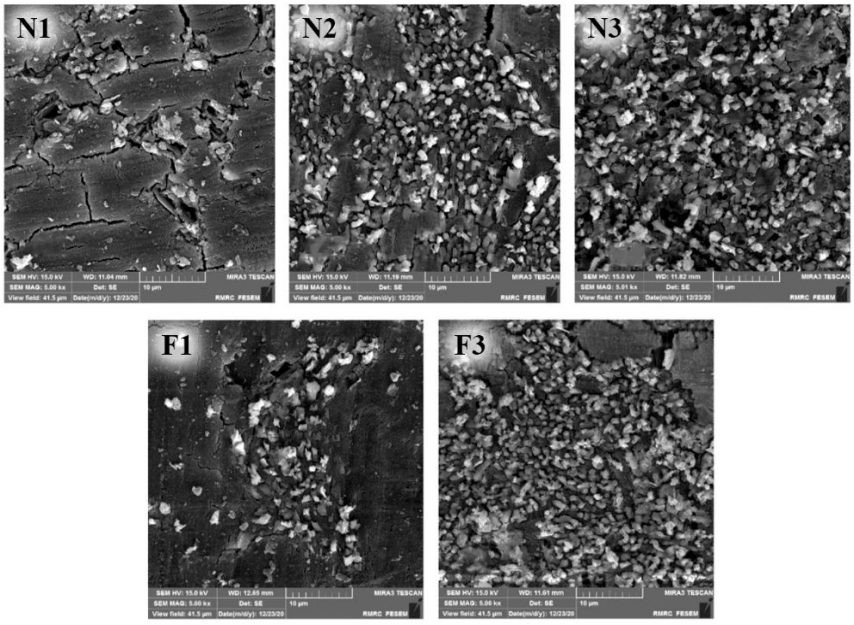

Fig. 6. Low-magnification FE-SEM micrographs of the samples.

However, excessive crystallization in certain compositions could still negatively influence transparency and surface gloss.

Fig. 8a & 8b present the EDS analyses obtained from the surface of the F3 sample corresponding to regions A and B marked in Fig. 7a. As observed, the results confirm the presence of the calcium aluminosilicate phase, identified as anorthite.

3.6. Optical and aesthetic properties

The optical characteristics of the prepared transparent borosilicate glazes were evaluated using gloss and CIE-Lab* colorimetric measurements. The gloss values together with the color parameters of the investigated glazes are summarized in Table 3.

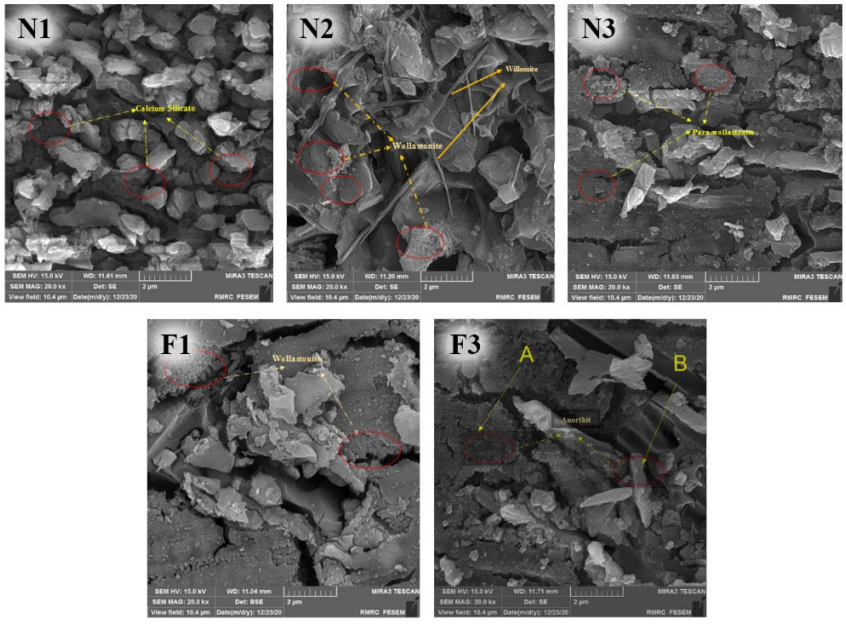

Fig. 7. High-magnification FE-SEM micrographs of the samples.

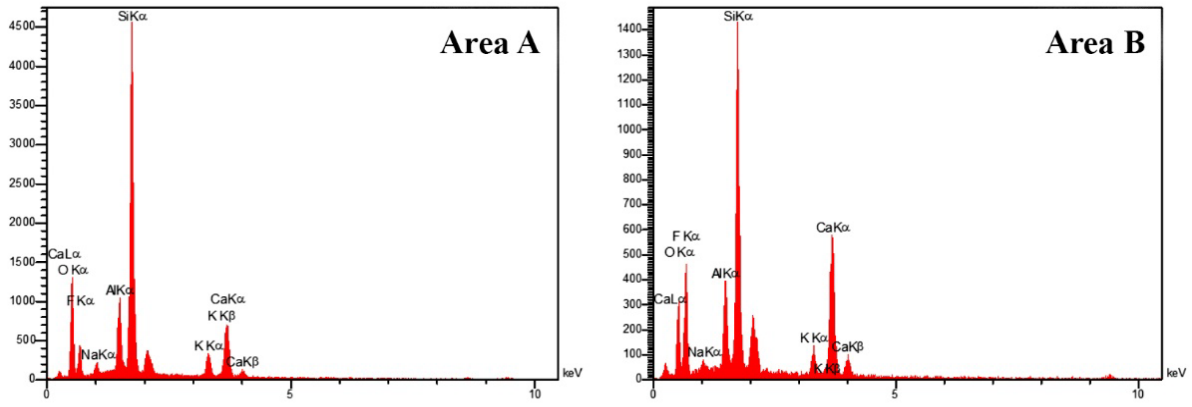

Fig. 8. The EDS analyses taken from the surface of the F3 sample in Fig. 7.

The optical behavior of the glazes was strongly dependent on the competition between viscous flow densification and crystallization during firing. In several nano-sized ZnO systems, improved densification and finer crystal distributions contributed to relatively homogeneous glaze surfaces. However, excessive crystallization in some compositions, particularly N3, increased light scattering and reduced surface gloss. These results indicate that the influence of nano-sized ZnO on transparency is composition-dependent and closely associated with the extent and morphology of crystalline phase formation. As observed, the F1 and F2 glazes exhibited relatively high gloss values, indicating the formation of smooth and highly reflective surfaces after firing. In contrast, the F3 and N3 samples showed significantly lower gloss values, which is consistent with the crystallization of calcium silicate phases within the glaze structure. The formation of crystalline phases such as wollastonite and anorthite reduced surface smoothness and increased light scattering, resulting in a whiter and more opaque appearance. The F3 and N3 samples exhibited lower gloss values compared with the F1 glaze. This behavior can be attributed to the development of crystalline phases including anorthite and wollastonite during firing. The crystallization process disrupted the continuity of the glassy matrix and increased surface roughness, thereby decreasing specular reflection from the glaze surface. Although the F2 glaze contained willemite as the dominant crystalline phase, the simultaneous formation of anorthite may also have contributed to the reduction in gloss compared with highly transparent systems. The coexistence of multiple crystalline phases increased optical heterogeneity within the glaze layer and influenced overall surface appearance.

The positive a* value observed for the F1 glaze corresponds to a light reddish tone on the glaze surface. Since the glazes were directly applied onto the ceramic substrate without an engobe layer, the use of a suitable white engobe could further improve the whiteness and brightness of the fired surfaces. The colorimetric results indicate that the investigated glaze systems exhibited varying degrees of opacity and surface brightness depending on phase composition and crystallization behavior during firing.

3.7. Microhardness

The Vickers microhardness values of the investigated glazes are summarized in Table 4. The hardness behavior was strongly dependent on the type of crystalline phases formed during firing as well as the amount of residual glassy phase.

As shown in Table 4, the F3 glaze exhibited the highest hardness value, which can be attributed to the formation of calcium aluminosilicate (anorthite) phases with relatively high intrinsic hardness [23]. The higher molar fraction of divalent cations in the residual glass phase may also contribute to the increased hardness of the F3 and N3 samples compared with the F2 and N2 systems.

In contrast, the lower hardness values of the F1 and N1 glazes can be related to their higher amorphous phase content, as confirmed by the XRD patterns, together with the presence of wollastonite phases, which possess lower hardness values (~ 400 HV). Overall, the hardness behavior of the investigated glazes was influenced by both crystalline phase composition and the relative fraction of residual glassy phase. Variations in crystal morphology, phase assemblage, and densification behavior collectively contributed to the observed mechanical performance.

Table 3. Gloss and CIE-Lab* colorimetric parameters of the investigated transparent borosilicate glazes.

Sample	c*	b*	a*	L*	Gloss
F1	11.27	−5.95	9.56	51.57	86.1
F2	1.77	0.47	1.70	74.41	83.2
F3	2.33	−0.04	2.33	76.53	67.30
N1	7.77	3.87	6.74	65.14	82.3
N2	6.02	2.64	5.41	68.05	84.3
N3	8.10	4.41	6.30	63.12	52.3

Table 4. Vickers microhardness values and crystalline phases of the investigated glazes fired at 1060 °C with a heating time of 90 min and soaking time of 3 min.

Sample	Microhardness (HV)	S ratio	Crystalline phase
F1	730 ± 14	0.38	Wollastonite
F2	744 ± 20	0.31	Willemite + calcium aluminosilicate
F3	817 ± 35	0.24	Calcium aluminosilicate
N1	755 ± 16	0.38	Calcium silicate
N2	635 ± 53	0.31	Willemite + wollastonite
N3	742 ± 42	0.24	Wollastonite

4. Conclusions

This study investigated the effect of ZnO particle size on the thermal behavior, phase evolution, microstructure, and optical properties of transparent borosilicate glass–ceramic glazes in the SiO_2–Al_2O_3–B_2O_3–ZnO–CaO–K_2O system. The results demonstrated that ZnO particle size significantly influences melting behavior, crystallization kinetics, and densification during firing. The nano-sized ZnO systems exhibited enhanced reactivity and promoted structural modifications within the glass network because of their higher surface area and improved dissolution behavior. DTA, FTIR, and XRD analyses indicated that finer ZnO particles influenced crystallization behavior and promoted the formation of finer and more homogeneous crystalline distributions compared with the micro-sized ZnO systems. FE-SEM observations confirmed noticeable differences in crystal morphology and microstructural homogeneity between the investigated glaze systems. The optical properties of the glazes were strongly dependent on the balance between viscous flow densification and crystallization. In several nano-sized ZnO systems, improved densification contributed to relatively homogeneous glaze surfaces, whereas excessive crystallization in certain compositions reduced gloss and increased optical scattering. The mechanical properties were also affected by phase composition and microstructural development during firing. Overall, the findings demonstrate that ZnO particle size is an important parameter for controlling crystallization behavior, surface quality, and microstructural evolution in transparent borosilicate glass–ceramic glazes.

CRediT authorship contribution statement

Raziye Salami: Conceptualization, Methodology, Writing – original draft.
Aida Faeghinia: Supervision, Funding acquisition.
Zahra Khakpour: Supervision, Writing – review & editing.
Mohammad Zakeri: Project administration, Resources.

Data availability

The data underlying this article will be shared on reasonable request to the corresponding author.

Declaration of competing interest

The authors declare no competing interests.

Funding and acknowledgment

The content of this article originates from a segment of the master's thesis of the first author, bearing project number 371397069. The authors wish to express their deep appreciation to the Materials and Energy Research Center (MERC) for their invaluable financial assistance.

Declaration of Generative AI and AI-assisted technologies in the writing process

The authors declare that ChatGPT (OpenAI GPT-5.5) was used for language editing, grammatical corrections, and stylistic improvement of this manuscript. Following the AI-assisted revisions, the authors carefully reviewed and edited the entire manuscript and take full responsibility for its accuracy, originality, and scientific content.

References

[1] F.G. Melchiades, B.T. Rego, S.M. Higa, H.J. Alves, A.O. Boschi, Factors affecting glaze transparency of ceramic tiles manufactured by the single firing technique, J. Eur. Ceram. Soc. 30 (2010) 2443–2449. https://doi.org/10.1016/j.jeurceramsoc.2010.04.030.
[2] S. Wang, X. Li, C. Wang, M. Bai, X. Zhou, et al., Anorthite-based transparent glass-ceramic glaze for ceramic tiles: Preparation and crystallization mechanism, J. Eur. Ceram. Soc. 42 (2022) 1132–1140. https://doi.org/10.1016/j.jeurceramsoc.2021.11.036.
[3] H. Gui, C. Li, C. Lin, Q. Zhang, Z. Luo, et al., Glass forming, crystallization, and physical properties of MgO-Al2O3-SiO2-B2O3 glass-ceramics modified by ZnO replacing MgO, J. Eur. Ceram. Soc. 39 (2019) 1397–1410. https://doi.org/10.1016/j.jeurceramsoc.2018.10.002.
[4] J. Choi, K. Kim, Crystallization behavior and microstructure of ZnO–Al2O3–SiO2–B2O3-based glass-ceramics using MgO and CaO modifiers, J. Non-Cryst. Solids. 646 (2024) 123230. https://doi.org/10.1016/j.jnoncrysol.2024.123230.
[5] P. Sahu, S. Musharaf Ali, K.T. Shenoy, A. Arvind, G. Sugilal, C.P. Kaushik, Combined experiments and atomistic simulations for understanding the effect of ZnO on the sodium silicate and sodium borosilicate glass network, J. Non-Cryst. Solids. 618 (2023) 122550. https://doi.org/10.1016/j.jnoncrysol.2023.122550.
[6] S.-M. Lee, S.-K. Kim, J.W. Yoo, H.-T. Kim, Crystallization behavior and mechanical properties of porcelain bodies containing zinc oxide additions, J. Eur. Ceram. Soc. 25 (2005) 1829–1834. https://doi.org/10.1016/j.jeurceramsoc.2004.06.009.
[7] N.V. Rudkovskaya, N.Y. Mikhailenko, Decorative Zinc-Containing Crystalline Glazes for Ornamental Ceramics (A Review), Glas. Ceram. 58 (2001) 387–390. https://doi.org/10.1023/A:1014958309094.
[8] F. Güngör, H. Çatır, M. Çakı, Investigation of the microstructural changes of a number of glazes after they are applied and fired on two different bodies, Boletín La Soc. Española Cerámica y Vidr. 59 (2020) 165–175. https://doi.org/10.1016/j.bsecv.2019.09.007.
[9] A.R. Jamaludin, S.R. Kasim, Z.A. Ahmad, The effect of CaCO3 addition on the crystallization behavior of ZnO crystal glaze fired at different gloss firing and crystallization temperatures, Sci. Sinter. 42 (2010) 345–355. https://doi.org/10.2298/SOS1003345J.
[10] M.O. Prado, E.D. Zanotto, Glass sintering with concurrent crystallization, C. R. Chim. 5 (2002) 773–786. https://doi.org/10.1016/S1631-0748(02)01447-9.

[11] J.J. Reinosa, F. Rubio-Marcos, E. Solera, M.A. Bengochea, J.F. Fernández, Sintering behaviour of nanostructured glass-ceramic glazes, Ceram. Int. 36 (2010) 1845–1850. https://doi.org/10.1016/j.ceramint.2010.03.029.
[12] H. Ali, S. Ali, K. Ali, S. Ullah, P.M. Ismail, et al., Impact of the nanoparticle incorporation in enhancing mechanical properties of polymers, Results Eng. 27 (2025) 106151. https://doi.org/10.1016/j.rineng.2025.106151.
[13] C. Tallon, M. Limacher, G.V. Franks, Effect of particle size on the shaping of ceramics by slip casting, J. Eur. Ceram. Soc. 30 (2010) 2819–2826. https://doi.org/10.1016/j.jeurceramsoc.2010.03.019.
[14] J.L. Amorós, E. Blasco, A. Moreno, N. Marín, C. Feliu, Effect of particle size distribution on the sinter-crystallisation kinetics of a SiO2–Al2O3–CaO–MgO–SrO glass-ceramic glaze, J. Non-Cryst. Solids. 542 (2020) 120148. https://doi.org/10.1016/j.jnoncrysol.2020.120148.
[15] L. Jiang, Y. Liao, Q. Wan, W. Li, Effects of sintering temperature and particle size on the translucency of zirconium dioxide dental ceramic, J. Mater. Sci. Mater. Med. 22 (2011) 2429–2435. https://doi.org/10.1007/s10856-011-4438-9.
[16] A. Wonisch, T. Kraft, M. Moseler, H. Riedel, Effect of Different Particle Size Distributions on Solid-State Sintering: A Microscopic Simulation Approach, J. Am. Ceram. Soc. 92 (2009) 1428–1434. https://doi.org/10.1111/j.1551-2916.2009.03012.x.
[17] M.A. Mahdy, I.K. El Zawawi, S.H. Kenawy, E.M.A. Hamzawy, G.T. El-Bassyouni, Effect of zinc oxide on wollastonite: Structural, optical, and mechanical properties, Ceram. Int. 48 (2022) 7218–7231. https://doi.org/10.1016/j.ceramint.2021.11.282.
[18] G.-H. Chen, X.-Y. Liu, Sintering, crystallization and properties of MgO–Al2O3–SiO2 system glass-ceramics containing ZnO, J. Alloys Compd. 431 (2007) 282–286. https://doi.org/10.1016/j.jallcom.2006.05.060.
[19] E. Ahmed, H.M. Aly, A.M. Abdelghany, A.A. Ismail, Structure and radiation shielding attitude of hexa-structured borosilicate glasses containing zinc oxide, Appl. Phys. A. 131 (2025) 401. https://doi.org/10.1007/s00339-025-08482-2.
[20] F.H. ElBatal, M.A. Marzouk, M.A. Azooz, H.A. Elbatal, Preparation of some selective glass–ceramics from nano-silica within the Li2O–SiO2 system with ZrO2 for future dental applications, Discov. Appl. Sci. 6 (2024) 156. https://doi.org/10.1007/s42452-024-05785-6.
[21] G. Acikbas, N. Calis Acikbas, N. Dizge, P. Belibagli, Multi-functional ceramic glazes with nano ZnO/Cu–ZnO incorporation, Ceram. Int. 50 (2024) 43800–43810. https://doi.org/10.1016/j.ceramint.2024.08.233.
[22] J. Cai, M. Lu, K. Guan, W. Li, F. He, et al., Effect of ZnO/MgO ratio on the crystallization and optical properties of spinel opaque glazes, J. Am. Ceram. Soc. 101 (2018) 1754–1764. https://doi.org/10.1111/jace.15321.
[23] M. Kavanova, Characterization of the interaction between glazes and ceramic bodies, Ceram. - Silik. 61 (2017) 267–275. https://doi.org/10.13168/cs.2017.0025.